Force fluctuations impact kinetics of biomolecular systems

Elena F. Koslover[1] and Andrew J. Spakowitz[1,2]
[1]*Biophysics Program, Stanford University, Stanford, California 94305, USA*
[2]*Chemical Engineering Department, Stanford University, Stanford, California 94305, USA*
(Received 12 July 2011; revised manuscript received 3 April 2012; published 10 July 2012)

A wide array of biological processes occur at rates that vary significantly with force. Instantaneous molecular forces fluctuate due to thermal noise and active processes, leading to concomitant fluctuations in biomolecular rate constants. We demonstrate that such fluctuations have a dramatic effect on the transition kinetics of force-dependent processes. As an illustrative, biologically relevant example, we model the pausing of eukaryotic RNA polymerase as it transcribes nucleosomal DNA. Incorporating force fluctuations in the model yields qualitatively different predictions for the pausing time scales when compared to behavior under the average force alone. We use our model to illustrate the broad range of behaviors that can arise in biomolecular processes that are susceptible to force fluctuations. The fluctuation time scale, which varies significantly for *in vivo* biomolecular processes, yields very different results for overall rates and dramatically alters the force regime of relevance to the transition. Our results emphasize the importance of transient high-force behavior for determining kinetics in the fluctuating environment of a living cell.

DOI: 10.1103/PhysRevE.86.011906 PACS number(s): 87.15.−v, 05.40.−a, 82.20.Pm

I. INTRODUCTION

The internal environment of a living cell is subject to a constant barrage of forces stemming from Brownian fluctuations, fluid flows, cytoskeletal deformation, and the action of molecular motors. Applied force is known to affect the kinetics of a variety of biologically relevant processes, ranging in scale from bond rupture [1–4] to motor stepping rates [5–7], genome structural rearrangements [8–10], and cell-cell adhesion [11]. Recent advances in single-molecule micromanipulation techniques have enabled researchers to directly map out the static force dependence of many such systems. However, the instantaneous force experienced by individual molecules *in vivo* is expected to fluctuate due to thermal motion and active biological processes. A quantitative understanding of transition rates within living cells thus requires consideration of force dynamics.

Previous treatments of kinetics under time-varying tension have focused primarily on externally imposed deterministic force trajectories [10,12,13]. Single-molecule studies of RNA hairpin unfolding have also investigated the roles of force variation along the reaction coordinate [14,15] and of thermal fluctuation of the force under a quasiequilibrium assumption that implies kinetic rates depend entirely on the average force [16–18]. In our work we employ a widely applicable method to examine reaction rates under forces that fluctuate stochastically on arbitrary time scales. We demonstrate that the fluctuation time scales play a critical role in determining effective rates and that transient excursions to high forces can dominate overall behavior. Our calculations underscore the need to quantify transition rates at high forces for understanding *in vivo* kinetics.

While the kinetic model presented here is applicable to a wide range of biologically relevant processes, we focus on an example system that illustrates some of the key points. Specifically, we develop a model for the pausing of eukaryotic RNA polymerase II (Pol II) as it transcribes nucleosomal DNA. Nucleosomes, which consist of DNA wrapped around an octamer of histone proteins, form the lowest level of organization in the hierarchic structure of eukaryotic chromatin. Pol II is known to enter into a long-lived pause state while transcribing through a nucleosome *in vitro* [19–21], and the rate of Pol II pausing as a function of force has been previously measured [22]. We develop a simple mechanical model for the polymerase and nucleosome system, which we use to estimate the forces experienced by Pol II at the nucleosome, and to calculate the expected rate of pausing during nucleosomal transcription. We show that the kinetics of Pol II pausing in this system are qualitatively affected by fluctuations in the force that arise from rapid wrapping and unwrapping of the nucleosome. This example system thus serves to demonstrate the importance of force fluctuation effects in a biologically relevant context.

II. GENERALIZED KINETIC MODEL

In this section we present a generalized model for computing transition times of a system under fluctuating force. Our model comprises a set of discrete states ($i = 1,2,\ldots,N$), with the molecular system experiencing a different force in each state. These states form a discretized landscape over which the system fluctuates with time distribution $P_{ij}(t)$ for transition between states i and j. At each state there is also a time distribution $P_{i*}(t)$ for a "reaction" to occur, which depends on the force at that state. For convenience, we define the cumulative distribution function $Q_i(t)$ as the probability that the particle remains in state i at time t after its arrival to that state,

$$Q_i(t) = 1 - \int_0^t \left[P_{i*}(t') + \sum_{j=0}^{N} P_{ij}(t') \right] dt'. \qquad (1)$$

To calculate the kinetics of the system, we first find the Green's function $G_{ij}(t)$, which gives the probability of finding a particle in state j at time t given it started in state i at

time 0:

$$G_{ij}(t) = \delta_{ij} Q_j(t) + \sum_{n=0}^{\infty} \sum_{i \xrightarrow{n} j} \int_0^t dt_n \int_0^{t_n} dt_{n-1} \ldots \int_0^{t_1} dt_0$$
$$P_{ik_1}(t_0) P_{k_1k_2}(t_1 - t_0) \ldots P_{k_nj}(t_n - t_{n-1}) Q_j(t - t_n). \quad (2)$$

Here the second summation goes over all paths from state i to state j with n intermediate states $(k_1, \ldots, k_n)$. The function G_{ij} assumes a convolution structure that is greatly simplified by taking a Laplace transform $t \to s$ in the time domain. The transformed function is given by

$$\widehat{G}_{ij}(s) = \delta_{ij} \widehat{Q}_j + \sum_{n=0}^{\infty} \sum_{i \xrightarrow{n} j} \widehat{P}_{ik_1} \widehat{P}_{k_1k_2} \ldots \widehat{P}_{k_{n-1}k_n} \widehat{P}_{k_nj} \widehat{Q}_j, \quad (3)$$

where the $\widehat{P}$, $\widehat{Q}$, are themselves the Laplace transforms of the corresponding distribution functions. The above expression is further simplified by considering the terms $\widehat{P}_{ij}$ as elements of a weighted adjacency matrix [23] $\widehat{\mathbf{P}}$ for transitions between states. The transformed Green's function is then expressed as

$$\widehat{G}_{ij}(s) = \sum_{n=0}^{\infty} (\widehat{\mathbf{P}}^n)_{ij} \widehat{Q}_j = [(\mathbf{I} - \widehat{\mathbf{P}})^{-1}]_{ij} \widehat{Q}_j. \quad (4)$$

While the numeric inversion of the Laplace transformed probability $\widehat{G}_{ij}(s)$ can be accomplished by equating the $\widehat{G}_{ij}$ to continued fractions and expanding around the poles [24], we concern ourselves here primarily with finding low-order moments in the time distribution for the reaction to take place. The average time for the particle starting in state i to undergo the reaction and leave the landscape is given by

$$\langle t_i \rangle = \int_0^{\infty} t \left[-\frac{\partial}{\partial t} \sum_{j=0}^{N} G_{ij}(t) \right] dt$$
$$= \int_0^{\infty} \sum_{j=0}^{N} G_{ij}(t) dt = \sum_{j=0}^{N} \widehat{G}_{ij}(s=0). \quad (5)$$

The variance in the reaction time can also be calculated by computing the second moment,

$$\langle t_i^2 \rangle = 2 \int_0^{\infty} \sum_{j=0}^{N} t G_{ij}(t) dt = \sum_{j=0}^{N} \frac{\partial \widehat{G}_{ij}}{\partial s} \Big|_{s=0}, \quad (6)$$

where the Laplace space derivatives are found via

$$\frac{\partial \widehat{G}_{ij}}{\partial s} = \left[(\mathbf{I} - \widehat{\mathbf{P}})^{-1} \cdot \frac{\partial \widehat{\mathbf{P}}}{\partial s} \cdot (\mathbf{I} - \widehat{\mathbf{P}})^{-1} \right]_{ij} \widehat{Q}_j$$
$$+ [(\mathbf{I} - \widehat{\mathbf{P}})^{-1}]_{ij} \frac{\partial \widehat{Q}_j}{\partial s}. \quad (7)$$

For any given starting distribution ρ_i of the system over the available states, the overall mean and variance of the reaction time can be found as $\langle t \rangle = \sum_i \langle t_i \rangle \rho_i$ and $\mathrm{var}(t) = \sum_i (\langle t_i^2 \rangle - \langle t_i \rangle^2) \rho_i$, respectively.

In addition to finding the time distribution for reaction in a fluctuating system, it is also of interest to calculate the distribution of states at which the reaction occurs. For a particle that starts in state i, the Laplace transformed time-distribution function for reaction from state j is

$$\widehat{R}_{ij}(s) = [(\mathbf{I} - \widehat{\mathbf{P}})^{-1}]_{ij} \widehat{P}_{j*}. \quad (8)$$

For initial distribution ρ_i, the overall probability that the reaction occurs from state j is then given by

$$\chi_j = \sum_i \rho_i \int_0^{\infty} R_{ij}(t) dt = \sum_i \rho_i \widehat{R}_{ij}(s=0). \quad (9)$$

The characteristics of a specific molecular system enter into this treatment through the time scales of fluctuation between different force states $[P_{ij}(t)]$, the force at each state (f_i), and the force dependence of the reaction time distribution $[P_{i*}(t) = P_*(f_i, t)]$. In the following sections we describe a physical model for the pausing of polymerase during nucleosomal transcription, which serves as an example of biologically relevant kinetics under fluctuating force.

III. MECHANICAL MODEL FOR POLYMERASE AND NUCLEOSOME SYSTEM

In order for a polymerase to transcribe through the nucleosome, downstream DNA must be rendered accessible by partially peeling off the nucleosome core. The amount of DNA wrapped on the nucleosome is believed to fluctuate rapidly [25]. If an insufficient length is unwrapped, the DNA must bend to accommodate the polymerase, resulting in a transient hindering force.

We develop a simple mechanical model of the polymerase and nucleosome system (Fig. 1), with the DNA treated as a semielastic chain wrapped around the nucleosome in a left-handed spiral. The parameters of the spiral are fit to the single nucleosome crystal structure [26]. The histone core of the nucleosome and the eukaryotic RNA polymerase Pol II are treated as hard spheres, with radii of 3.2 and 5 nm, respectively.

The "linker" DNA unwrapped from the nucleosome has one end position and orientation fixed to match up to the bound spiral. We discretize the linker chain into $M = 30$ segments and define the energy function for any given configuration as a combination of quadratic stretching and bending energies:

$$\frac{E_{\mathrm{conf}}}{kT} = \frac{\kappa_s}{2\ell_0} \sum_{i=1}^{M} (|\vec{v}_i| - \ell_0)^2 + \frac{\ell_p}{\ell_0} \sum_{i=1}^{M} \left[1 - \frac{\vec{v}_i \cdot \vec{v}_{i+1}}{|\vec{v}_i||\vec{v}_{i+1}|} \right], \quad (10)$$

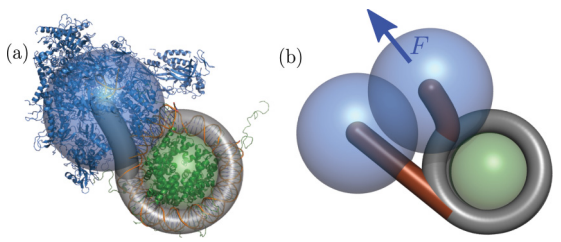

FIG. 1. (Color) Mechanical model for polymerase transcribing through a nucleosome. (a) Pol II (blue), histone core (green), and DNA (gray) are shown superimposed on crystal structures. (b) Optimized configurations for different lengths of DNA unwrapped ahead of the polymerase. Linker DNA (brown) is bend for short lengths. Arrow indicates hindering force on the polymerase.

where $\vec{v}_i$ is the vector corresponding to the ith segment, $\ell_0 = L/N$ is the ground-state segment length, L is the length of unbound DNA, $\kappa_s = 268\,\mathrm{kT/nm}$ is the stretch modulus, and $\ell_p = 50\,\mathrm{nm}$ is the persistence length for double-stranded DNA.

Numeric optimization is used to find the lowest energy path for a given length of unpeeled DNA, subject to the constraint that the free end must remain at least 8.2 nm from the nucleosome center. This constraint is equivalent to assuming that the unwrapped DNA passes through the polymerase center, while modeling the interaction between polymerase and nucleosome as hard-sphere steric exclusion. The resulting configurations of the linker are illustrated in Fig. 1(b). We note that for $L > 21\,\mathrm{bp}$, the unbound DNA can be fully straightened without steric interference of the nucleosome and the polymerase so that above these lengths, $E_{\mathrm{conf}}(L) = 0$.

The overall energy for a state where length L of DNA is unpeeled in front of the polymerase also includes the energy change associated with straightening the DNA out of the spiral configuration and the loss of binding energy to the nucleosome:

$$E(L) = E_{\mathrm{conf}}(L) + \left(\frac{kT(2\pi)^4 \ell_p R^2}{2L_T^4} - \phi\right)(L_{\mathrm{tot}} - L), \quad (11)$$

where $L_T = \sqrt{(2\pi R)^2 + h^2)}$ is the length per spiral turn, $L_{\mathrm{tot}} = 147\ \mathrm{bp} \times 0.34\ \mathrm{nm/bp}$ is the total length of nucleosomal DNA, and $\phi = 2.17\ \mathrm{kT/nm}$ is the estimated binding strength for DNA on the nucleosome [27].

The force exerted on the polymerase by the nucleosome is equivalent to the force required to bend the unwrapped DNA into its optimal configuration. Thus, $F(L) = |\nabla E_{\mathrm{conf}}(L)|$ if the optimized structure hits the constraint boundary for the minimum distance between polymerase and nucleosome centers, and $F(L) = 0$ otherwise.

This mechanical model defines an energy landscape for the system as a function of the unwrapped linker length (Fig. 2).

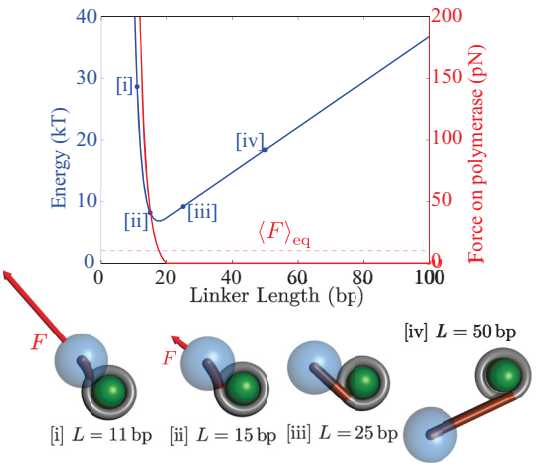

FIG. 2. (Color) Energy $E(L)$ (blue) and force $F(L)$ on Pol II (red) as a function of the length of DNA unwrapped ahead of the polymerase. Dashed line indicates force averaged over all linker lengths. Sample configurations for different linker lengths are illustrated, with red arrows indicating magnitude and direction of force.

For short linkers, the free DNA chain bends to accommodate the polymerase, sharply increasing the configuration energy. In this case, the nucleosome exerts a hindering force on the polymerase that is just strong enough to bend the DNA. In contrast, long lengths of linker DNA straighten upon unbinding. However, the release of mechanical strain is offset by the energy penalty due to loss of binding interactions. For purposes of our kinetic calculations, the landscape is broken up into discrete states corresponding to the number of base pairs unwrapped from the nucleosome, with energy E_L and force F_L associated with each state.

IV. KINETIC MODEL FOR POLYMERASE AND NUCLEOSOME SYSTEM

The kinetics of our model system consist of fluctuations in the length of DNA unwrapped ahead of the polymerase, with the force at different linker lengths modulating the rate of pausing at that state (Fig. 3). For simplicity, we assume the waiting times for all transitions to be exponentially distributed. The Laplace-transformed transition matrix $\widehat{\mathbf{P}}$ is tridiagonal, with

$$\widehat{P}_{L,L-1} = \frac{k_L^{(w)} + k^{(s)}}{s + k_L^{(u)} + k_L^{(w)} + k_L^{(p)} + k^{(s)}},$$
$$\widehat{P}_{L,L+1} = \frac{k_L^{(u)}}{s + k_L^{(u)} + k_L^{(w)} + k_L^{(p)} + k^{(s)}}, \quad (12)$$

and the transformed distribution of pausing times is

$$\widehat{P}_{L*} = \frac{k_L^{(p)}}{s + k_L^{(u)} + k_L^{(w)} + k_L^{(p)} + k^{(s)}}, \quad (13)$$

where the $k_L^{(u/w)}$ are the rates for unwrapping and rewrapping of the nucleosomal DNA, $k^{(s)}$ is the forward-stepping rate of the polymerase, and $k_L^{(p)}$ is the pausing rate. The rate constants are estimated from the mechanical model as described below.

The amount of unwrapped DNA is assumed to fluctuate diffusively over the energy landscape defined in the previous section. An uphill step should occur at a rate that decreases exponentially with the energy difference, while the rate of downhill stepping under fluid drag must exhibit a linear increase down a large energy gradient. Solution of the discretized Fokker-Planck equation yields the following expression for the rate of unwrapping and rewrapping a single base pair [28,29]:

$$k_L^{(u/w)} = \frac{R_0(E_{L\pm1} - E_L)}{\exp(E_{L\pm1} - E_L) - 1}, \quad (14)$$

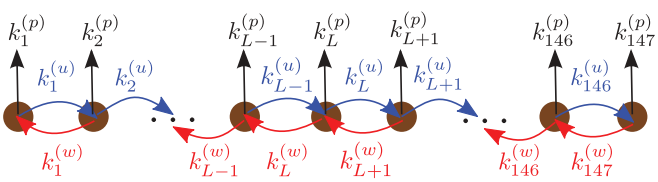

FIG. 3. (Color online) Schematic of discrete state model for linker DNA length fluctuations and polymerase pausing. $k^{(s)}$ is the polymerase stepping rate, $k^{(u/w)}$ are the rates for unwrapping and rewrapping a single base pair, and $k^{(p)}$ is the pause rate.

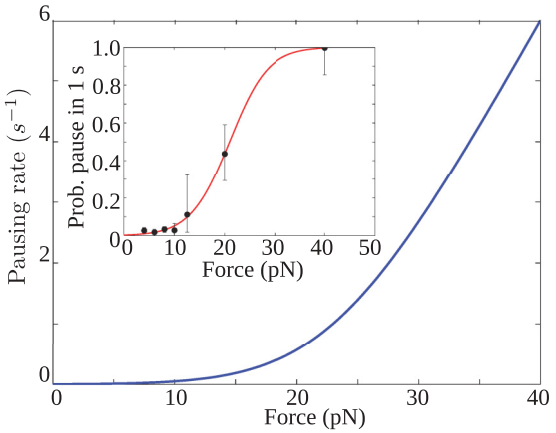

FIG. 4. (Color online) Pol II pausing rate as a function of force, from fit to experimental data [22] (inset).

where E_L is the energy (in units of k_BT) at linker length L, and R_0 is a fundamental fluctuation rate.

As the length of unwrapped DNA fluctuates, the force experienced by the polymerase changes. To model the dependence of Pol II pausing rates on force, we use single-molecule force spectroscopy data published by Galburt *et al.* [22]. We fit the data for pause rates under hindering load to the following generalized expression for force-dependent transition rates:

$$k^{(p)}(F) = \frac{D}{k_BT}\frac{FL-U}{2L^2}\frac{\exp[(FL-U)/2k_BT]}{\sinh[(FL-U)/2k_BT]}. \quad (15)$$

This expression is derived from coarse-grained solution of the Fokker-Plank equation on a piece-wise linear approximation of the potential [29]. Here, D is the local diffusion coefficient, U is the potential barrier for the transition, and L is the length of the transition step in the reaction coordinate conjugate to the force F. The expression $\mathcal{P}(F) = 1 - \exp[-k^{(p)}(F)\Delta t]$, with $\Delta t = 1\,\mathrm{s}$ is fit directly to the data of Galburt *et al.* for the probability of pausing within a 1-s interval (Fig. 4). The parameters corresponding to the optimum fit are $D = 1.76\,\mathrm{nm}^2/\mathrm{s}$, $L = 1.4\,\mathrm{nm}$, and $U = 7.7k_BT$. Plugging these parameters into Eq. (15) yields the force dependence of the pausing rate (Fig. 4) used in our kinetic calculations. Given the small number of available data points for fitting a three-parameter model, we also consider the range of possible parameter values that would be consistent with experimental data (see Appendix A).

We note that any single-molecule measurement designed to measure transition rates under force will itself be subject to thermal force fluctuations, which should be taken into consideration when interpreting results [30]. When extracting force-dependent pause rates $[k^{(p)}(F)]$ from optical tweezer data, it is assumed that fluctuations of the experimental system from the average reported force are not sufficiently large to affect the polymerase kinetics. This assumption is validated in Appendix B by calculating that the force distributions in an optical trap are much narrower than the distribution of forces that is experienced by the polymerase while transcribing a nucleosome.

The transition time distributions given by Eq. (13) fully describe our kinetic model for the polymerase and nucleosome system. While the discrete kinetic model is fully solvable analytically, we employ dynamic Monte Carlo simulations using the Gillespie algorithm [31] to illustrate system trajectories in limiting regimes. In the discussion below, the effective pausing rate for the polymerase in this fluctuating system is defined as the inverse of the mean first passage time to reaction, $k_{\mathrm{eff}}^{(p)} = 1/\langle t\rangle$, where $\langle t\rangle$ is found using Eq. (5).

V. RESULTS AND DISCUSSION

The hindering force experienced by Pol II, averaged over all Boltzmann-weighted fluctuations in the linker length, is given by

$$\langle F\rangle_{\mathrm{eq}} = \frac{\sum_{L=0}^{147} F_L \exp(-E_L)}{\sum_{L=0}^{147}\exp(-E_L)} \approx 5\,\mathrm{pN}. \quad (16)$$

We note that at this force, the average time to enter into the pause state is $1/k^{(p)}(\langle F\rangle_{\mathrm{eq}}) \approx 80\,\mathrm{s}$. The pause-free velocity of Pol II is approximately 12 bp/s [22]. Thus, based on the average hindering force alone, the polymerase would be able to transcribe all the way through the 147 bp of the nucleosome without pausing. A static model incorporating only the average force is thus insufficient to explain the tendency of Pol II to pause during nucleosomal transcription [21].

In the fluctuating environment of the cell, the instantaneous force experienced by the polymerase can be significantly higher than the 5 pN average. The overall rate of pausing depends on the time scales for sampling over the instantaneous forces. Our general kinetic model presented in Sec. II offers a convenient formalism for calculating the low-order moments of the reaction time distributions. Here, we calculate the average time to pausing using Eq. (5) applied to our specific mechanical model.

Figure 5 illustrates the key role played by the underlying fluctuations in determining the overall kinetics of our polymerase-nucleosome model. We provide results for a range of fluctuation rates R_0 in order to illustrate the various behaviors at different regimes before specializing our discussion to the specific experimental parameters of the nucleosome and polymerase. For rapid fluctuations, the length of unwrapped DNA remains equilibrated, with the force experienced by the polymerase sampled over a wide range of values [Figs. 6(a)–6(c)]. The overall rate of pausing thus approaches the average rate $k_{\mathrm{eff}}^{(p)} \to \langle k^{(p)}\rangle_{\mathrm{eq}} \approx 0.09\,\mathrm{s}^{-1}$. This rate is significantly faster than the pausing rate at the average force, $k^{(p)}(\langle F\rangle_{\mathrm{eq}}) \approx 0.01\,\mathrm{s}^{-1}$. Furthermore, in the fast fluctuation regime, the polymerase pauses on average while experiencing a 24–pN hindering force [Fig. 5(b)]. The pausing behavior of the polymerase in this regime is thus dictated by forces far above the equilibrium average.

In the extreme of very slow unwrapping fluctuations, polymerase pausing can occur at much lower rates. Specifically, in a static system where the polymerase does not step forward and the linker length remains constant, the time to pause is averaged over all states, yielding the effective rate $k_{\mathrm{eff}}^{(p)} \to \langle 1/k^{(p)}\rangle_{\mathrm{eq}}^{-1} \approx 0.006\,\mathrm{s}^{-1}$. In this regime, the average force at the point of pausing is equal to $\langle F\rangle_{\mathrm{eq}}$ if the system is initiated at equilibrium.

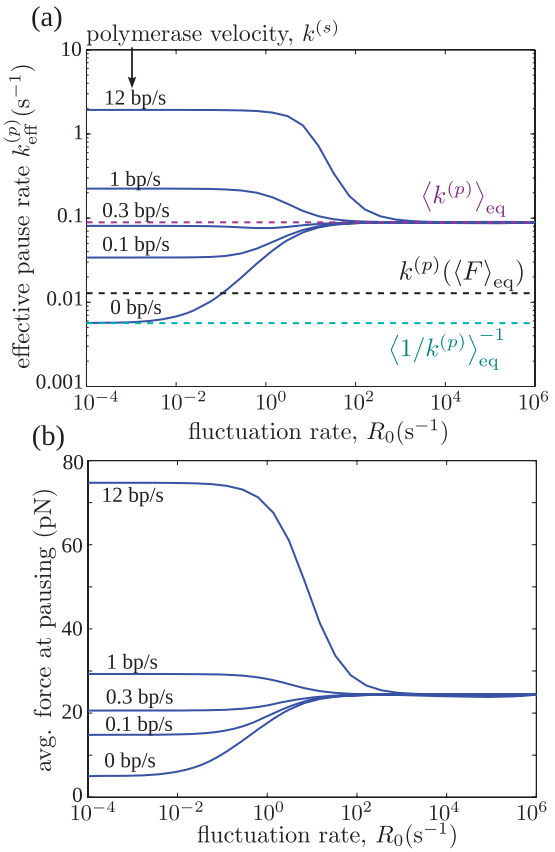

FIG. 5. (Color) (a) Effective polymerase pausing rate [$k_{\rm eff}^{(p)}$] as a function of nucleosome unwrapping fluctuation rate, plotted for different stepping velocities. Dashed lines indicate asymptotic results for slow (cyan) and fast (magenta) fluctuations, as well as the pause rate at average force (black) for comparison. (b) Average force experienced by the polymerase at the point of pausing.

The kinetics of polymerase stepping towards the wrapped portion of the nucleosome also has a defining role to play in determining pausing behavior. When unwrapping fluctuations are much faster than the stepping rate $k^{(s)}$, the length of linker DNA remains equilibrated and the effective pausing rate is independent of $k^{(s)}$. However, if the polymerase moves forward quickly enough that the downstream DNA does not have enough time to equilibrate, then the linker is bent more tightly with each step [Fig. 6(e)]. The pausing time is then roughly equal to the time required for the polymerase to progress towards a high-force barrier. The most frequent pausing is seen in the regime of rapid polymerase stepping and slow relaxation of the downstream DNA. The rapid pausing as the polymerase steps towards higher forces is apparent in trajectories obtained from dynamic Monte Carlo simulations of the system [Fig. 6(d)].

Our results emphasize the importance of both fluctuation rates and the rate of directed stepping over an energy landscape in determining kinetics of a force-dependent transition. The regime occupied by a specific biomechanical system must be determined from independent measurement of the relevant rates. The fundamental rate R_0 for thermal unwrapping of a single nucleosomal base pair can be extracted from single-molecule unpeeling experiments [27] and kinetic accessibility [25] data. This rate is estimated as 10^4–$10^6\,s^{-1}$ (see Appendix C). The system of Pol II transcribing through a nucleosome thus lies in the regime of rapid fluctuations.

Our calculations imply an average time of 11 s for Pol II to enter a pause state while on the nucleosome. We note that the paucity of data for Pol II pausing at high forces allows for a wide range of possible fits for $k^{(p)}$ as a function of force (Appendix A). The corresponding average times to pause in the fast fluctuation regime fall in the range of 0.03 to 17 s, which includes the experimentally measured average time of 4 s [21]. The wide range of possible effective pausing rates highlights the importance of polymerase behavior at high forces ($F > 10$ pN). Regardless of the precise rate, we find that Pol II has a high chance of pausing during the ∼12 s required to fully transcribe through a nucleosome. This result is in agreement with *in vitro* observations of polymerase pausing during nucleosomal transcription [19–21].

We emphasize that our simple physical model for nucleosomal transcription by Pol II is not intended to fully encompass the details of this complicated biomechanical process. For instance, the effects of DNA twist and electrostatic interactions between polymerase and nucleosome are not included. The action of Pol II involves the unzipping of DNA, resulting in the potential buildup of twist deformation within a topologically closed supercoiling domain [32]. This effect could result in additional fluctuating forces and torques felt by the polymerase, further modulating the effective processive behavior. However, our simplified model system serves to illustrate the impact of force fluctuations on the pausing kinetics, and additional effects can be incorporated into this framework in future studies. Overall, a static system incorporating the average force alone yields very slow rates of pausing, whereas by considering fluctuation effects we are able to obtain an approximate estimate of the pausing rate that is consistent with *in vitro* results.

VI. CONCLUDING REMARKS

The alteration of kinetics as a result of force fluctuations is expected to apply far beyond the polymerase-nucleosome example. Other biomolecular transitions can explore entirely different regimes of the relevant rates. For instance, large vesicles carried through the cytoplasm by kinesin molecules would exert slowly fluctuating forces on the motor. Processes requiring large-scale DNA rearrangements, such as formation of loops for assembly of transcription factor complexes, will be subject to thermal noise on the millisecond time scale [10]. Fluctuations in tension on cell-cell adhesion bonds due to whole-cell dynamics would lie in an even slower regime. In addition to thermal fluctuations, relaxation processes following the action of any biomechanical motor would also yield time-varying forces that can alter the kinetics of subsequent steps.

Our results reveal a broad range of kinetic behaviors over the biologically relevant fluctuation-rate spectrum, and our approach facilitates a rapid calculation of transition kinetics for arbitrary fluctuation and stepping time scales. This work highlights the importance of high-tension behavior in the kinetics of biomolecules in a fluctuating environment. Force-dependent transitions can be highly sensitive to brief excursions into the large force regime. For our example

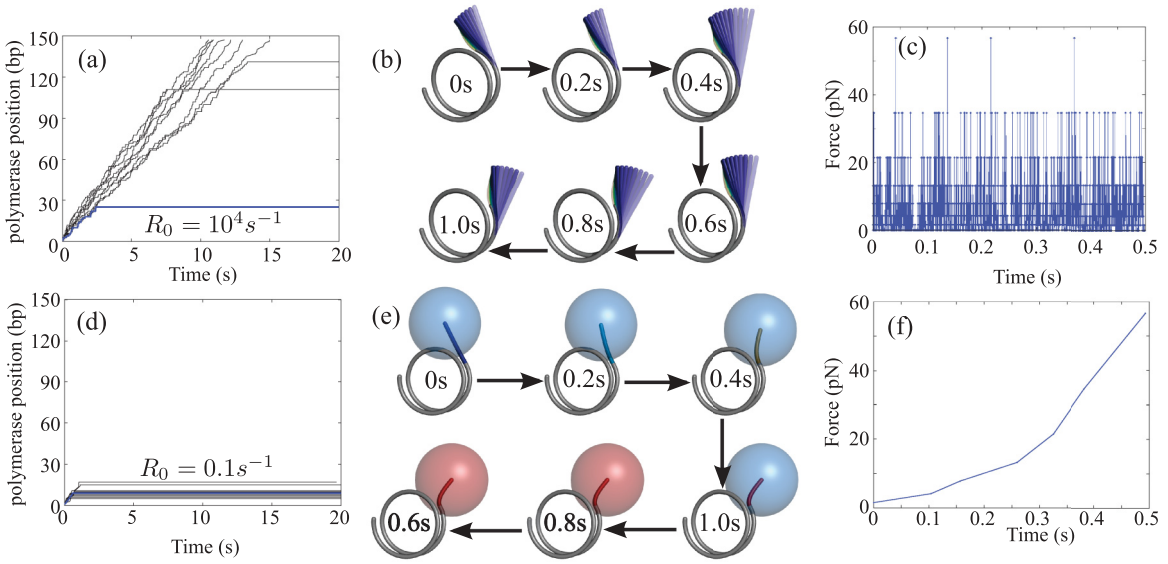

FIG. 6. (Color) (a) Sample traces from dynamic Monte Carlo simulations of polymerase and nucleosome system, with rapid unwrapping of nucleosome ($R_0 = 10^4\,\mathrm{s}^{-1}$). (b) Illustrated states for single sample trajectory, with all states accessed during a 0.02-s interval overlaid. Transparency is proportional to the amount of time spent in the state, and color is proportional to force. (c) Force experienced by polymerase over a sample trajectory. (d)–(f) Corresponding figures for slow nucleosome unwrapping ($R_0 = 0.1\,\mathrm{s}^{-1}$). Red polymerase color indicates paused state.

system of Pol II transcribing through a nucleosome, entry into the pause state is predicted to occur at a much higher force and a much faster rate than expected for a static system. The spectrum of force fluctuations arises from the elastic response of the biomolecular system. The considerable molecular rigidity at the nanoscale level translates to large force fluctuations that significantly impact kinetics. Our model of Pol II transcribing through nucleosomal DNA typifies these general effects. Investigating the time scale and magnitude of force fluctuations in an *in vivo* environment, as well as the response of biomolecules to these fluctuations, is critical to developing a quantitative picture of kinetics in a living cell.

ACKNOWLEDGMENTS

We thank S. Mehraeen for sharing trap fluctuation results ahead of publication and D. J. Koslover for fruitful discussions. This research was supported by funding from the Hertz Foundation and the NSF CAREER Award Program.

APPENDIX A: PARAMETER RANGE FOR FORCE DEPENDENCE OF PAUSE RATES

To model the dependence of Pol II pausing rates on force, we fit a three-parameter function [Eq. (15)] to single-molecule force spectroscopy data published by Galburt *et al.* [22]. Given the small number of available data points and large error bars, we also consider the range of possible parameter values that would be consistent with the experimental data. Specifically, we assume that the diffusive sampling rate D relevant to the transition into the pause state is limited to lie below the free diffusion coefficient of Pol II ($4 \times 10^7\,\mathrm{nm}^2/\mathrm{s}$ for a 5-nm sphere). With this limitation we find the two extreme sets of D, L, U parameters that minimize and maximize the effective pausing rate in the rapid fluctuation limit $k_{\mathrm{eff}}^{(p)} = \langle k^{(p)} \rangle_{\mathrm{eq}}$, under the constraint that the force-dependence curve must fit within the error bounds of the experimental data [Fig. 7(a)]. These two extreme fits yield values of $\langle k^{(p)} \rangle_{\mathrm{eq}} = 0.06\,\mathrm{s}^{-1}$ and $\langle k^{(p)} \rangle_{\mathrm{eq}} = 30\,\mathrm{s}^{-1}$. The effective pausing rates for different fluctuation time scales can thus vary over several orders

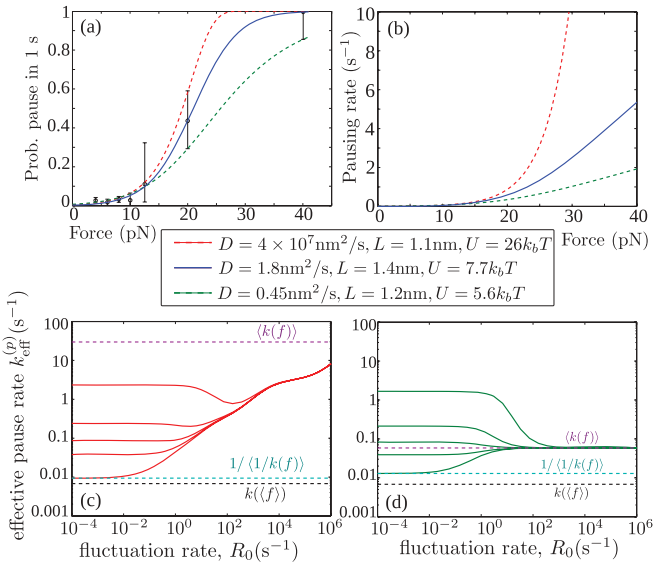

FIG. 7. (Color online) Determining Pol II pausing rates as a function of force. (a) Fits to experimental data. Best fit shown as solid curve. Dashed curves give fits that fall within error bars but yield extreme values of the effective pausing rate in the rapid fluctuation regime. (b) Pausing rates as a function of force, for the three fitting curves. (c) Effective pausing rates for different values of the polymerase speed $k^{(s)}$ (top to bottom: 12 bp/s, 1 bp/s, 0.3 bp/s, 0.1 bp/s, and 0 bp/s) for the upper extreme fit part (a). (d) Effective pausing rates for the lower extreme fit in part (a). The corresponding plot for the best fit is shown in Fig. 3(b).

of magnitude without departing from the experimental data [Figs. 7(c) and 7(d)].

Since the uncertainty in the experimental measurements occurs primarily in the high-force regime ($F > 10$ pN), the wide range of possible effective pausing rates demonstrates the importance of obtaining accurate measurements at tensions well above the *in vivo* average in order to gain a quantitative understanding of transition kinetics in the presence of fluctuations.

APPENDIX B: FORCE FLUCTUATIONS IN SINGLE-MOLECULE RATE MEASUREMENTS

When pausing rates are measured in a single-molecule experiment, the polymerase is subject to fluctuations in the force that arise from thermal motion of the bead in the optical trap. Given the momentous impact of such fluctuations in the biologically relevant case of RNAP transcribing through a nucleosome, the question arises as to whether force fluctuations in the trap would significantly alter the observed rate constants. In such a case, extracting the pausing kinetics from the experimental measurements would require a correction for the effect of fluctuations. Prior studies of biomolecular kinetics in an optical trap have investigated the role of thermal fluctuation in the force using thermodynamic quasiequilibrium assumptions [16–18]. Here we address this question by employing our previously developed model for the distribution of forces experienced by DNA in an optical trap [30].

For a DNA handle of length L, which is fixed at one end and at the other end attached to a bead of radius a, the partition function corresponding to the end-to-end vector $\vec{R}_D$ is given by

$$G(\vec{R}_D) = \int d\vec{u}\, G_{\rm wlc}(\vec{R}_D; L) \times \exp\left[-\frac{\kappa}{2k_bT}(\vec{R}_D + a\vec{u} - \vec{R}_T)^2\right], \quad \text{(B1)}$$

where $G_{\rm wlc}$ is the wormlike chain partition function with fixed end points [24], $\vec{R}_T$ is the position of the trap center, $\vec{u}$ is the orientation of the bead, and κ is the trap stiffness. In our calculations, we use the parameters $\kappa = 0.05$ pN/nm, $L = 9$ kbp, and $a = 2.1$ μm as reported by Galburt *et al.* [22]. We define the $\hat{z}$ axis as pointing from the fixed DNA end to the trap center. Since $G_{\rm wlc}$ depends only on the DNA end-to-end distance, Eq. (B1) can be employed to find both P_D (the probability density for the separation distance between the DNA ends) and P_z (the probability density for the position of the bead center along the $\hat{z}$ axis) [30]. Specifically, these densities can be expressed as

$$P_D(D) = \frac{D^2}{\mathcal{N}_D}\exp(-\beta\kappa D^2/2)G_{\rm wlc}(D; L) \times \int_{-1}^{1} d\rho_D\, d\rho_u\, I_0\left(\beta\kappa a D\sqrt{1-\rho_D^2}\sqrt{1-\rho_u^2}\right) \times \exp[\beta\kappa(a|R_T|\rho_u + D|R_T|\rho_D - aD\rho_D\rho_u)] \quad \text{(B2)}$$

$$P_z(z) = \frac{1}{\mathcal{N}_z}\int_{-1}^{1} d\rho_u \int_0^{\sqrt{L^2-(z-a\rho_u)^2}} dy\, y\, I_0(\beta\kappa a y\sqrt{1-\rho_u}) \times G_{\rm wlc}(\sqrt{y^2+(z-a\rho_u)^2}; L) \times \exp\left\{-\frac{\beta\kappa}{2}[(|R_T|-z)^2 + y^2]\right\}, \quad \text{(B3)}$$

where $\beta = 1/k_BT$, I_0 is the zeroth-order modified Bessel function, and $\mathcal{N}_D$,$\mathcal{N}_z$ are normalization constants.

For each position of the trap $\vec{R}_T$, the force reported in a single-molecule experiment is given by the average trap force $\langle F_z\rangle = \kappa(|R_T| - \langle z\rangle)$, where the average position of the bead center $\langle z\rangle$ can be calculated using the distribution given in Eq. (B3). The end-to-end force experienced by the DNA tether at an extension D is obtained through the Legendre transform, $F = -k_BT\,\partial\log[G_{\rm wlc}(D; L)]/\partial D$, and the distribution of forces can thus be derived from Eq. (B2).

Carrying out the appropriate integrals and derivatives numerically yields the distributions of forces experienced by the polymerase at different positions of the trap [Fig. 8(a)]. We note that by comparison to the force while transcribing through a nucleosome, the forces experienced in the trap are much more

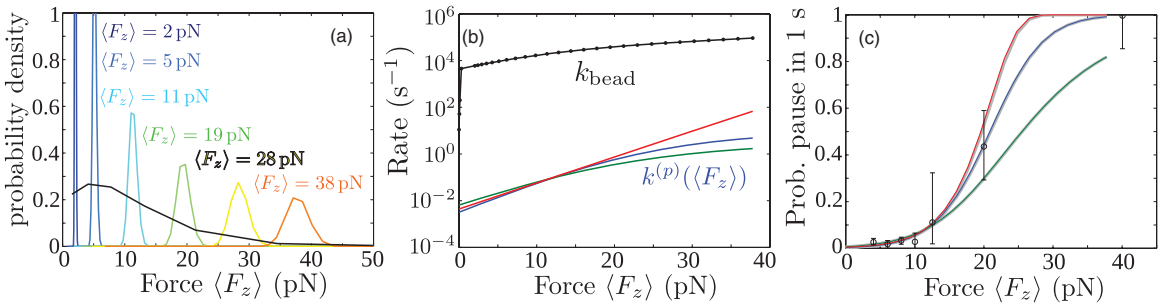

FIG. 8. (Color) (a) Colored lines indicate distributions of the force experienced by the DNA tether at different trap positions. The average trap force corresponding to each position is indicated. The black line indicates distribution of forces experienced by the RNAP while transcribing through a nucleosome, according to the model described in this work. (b) Rates of polymerase pausing under force. Red, blue, and green curves correspond to three fits of the experimental data (Fig. 7); black curve plots $k_{\rm bead}$, the rate constant for the bead in the optical trap to diffuse a distance corresponding to the width of the distance distribution, at each trap position. (c) Probability of RNAP pausing in a 1-s interval, as a function of average trap force. Red, blue, and green lines are predictions based on the parameter fits in Fig. 7, taking into account rapid fluctuations in the force experienced by the DNA in the trap ($1 - \exp[\langle k^{(p)}(F)\rangle]$). For comparison, grey lines show the corresponding curves based on the average force ($1 - \exp[k^{(p)}(\langle F_z\rangle)]$).

narrowly distributed, indicating that force fluctuations should have less of an effect on the rate constants measured in the single-molecule experiment.

In order to understand the effect of the force fluctuations on kinetics in the optical trap, we must consider the time scale associated with the fluctuations. We thus calculate the fundamental rate $k_{\text{bead}}(F)$ associated with moving the bead by a distance comparable to the width of the distribution P_D; motion of this magnitude would be required to significantly affect the force experienced by the RNAP. We use the approximation $k_{\text{bead}} = 2D_{\text{bead}}/\sigma^2$, where $D_{\text{bead}} \approx 2 \times 10^5\ \text{nm}^2/s$ is the bead diffusion constant and σ is the standard deviation of the distribution in end-to-end distances P_D. We find that the time scale associated with fluctuations of the bead in the optical trap is at least three orders of magnitude shorter at all trap positions than the time scale for polymerase pausing, so that the system falls distinctly in the fast fluctuation regime [Fig. 8(b)].

In the fast fluctuation limit, the pausing rate should approach the average rate $\langle k^{(p)}(F)\rangle$. We find that this average rate, which incorporates fluctuation in the force, gives very similar results for RNAP pausing kinetics in the optical trap as the rate at the average trap force $k^{(p)}(\langle F_z\rangle)$ [Fig. 8 (c)]. Thus, fluctuations in the force are not expected to have a significant effect on the optical trap data reported by Galburt *et al.* [22]. For this system, force fluctuations in the optical trap are sufficiently small that force-dependent kinetics can be extracted directly by assuming only the average force is experienced by the polymerase.

APPENDIX C: RATES OF NUCLEOSOME UNWRAPPING

We parametrize the time scale for unwrapping fluctuations of the nucleosome by the fundamental rate of attempting to unpeel a single base pair [R_0 in Eq. (14)]. This rate is equivalent to the diffusion constant of the underlying motion expressed in units of bp^2/s [28]. We previously developed a mechanical model for nucleosome unwrapping under tension, which was fit to single-molecule force-extension measurements of a mononucleosome [27]. Dynamic simulations with this model allowed us to extract a rate constant of $R_0 = 4 \times 10^6\ \text{s}^{-1}$ for the unpeeling process.

Other experimental results that shed light on the fluctuation rate include kinetic measurements of protein binding to sites that are temporarily revealed upon nucleosome unpeeling, as well as fluorescence correlation spectroscopy (FCS) results with a fluorophore attached to the bound DNA edge [25]. Our generalized theory for transition rates of a fluctuating system can easily be applied to the unpeeling of a free nucleosome in order to calculate the average time required for a LexA protein to bind to its target site located 8 to 27 base pairs from the nucleosome edge, as measured by Li *et al.* [25]. The experimentally measured average time is $\tau_{\text{expt}} = 0.25\,\text{s}$. For this system, the energy of each state is given by

$$E(L) = \left(\frac{kT(2\pi)^4 \ell_p R^2}{2L_T^4} - \phi\right)(L_{\text{tot}} - L), \qquad \text{(C1)}$$

corresponding to the nucleosomal part of the energy defined in Eq. (11). The rate of individual wrapping and unwrapping steps is given by Eq. (14) using this energy function. We assume that in order for the LexA to bind the entire site must be unwrapped and that the binding process itself is very fast. Thus, we take $P_{i*} = 0$ for $i < 27$, and $P_{i*} = \infty$ otherwise. Plugging this system into our general model for fluctuating kinetics allows us to fit the fundamental rate constant $R_0 = 4 \times 10^4\ \text{s}^{-1}$ in order to obtain an average binding time $\langle t\rangle = 0.25\,\text{s}$ comparable with the experimentally measured value.

Results from these two experiments thus indicate that the fluctuation rate for nucleosome unwrapping falls in the $R_0 = 10^4$–$10^6\ \text{s}^{-1}$ range and so places our polymerase and nucleosome system in the rapid fluctuation regime.

[1] A. Wiita, S. Ainavarapu, H. Huang, and J. Fernandez, Proc. Natl. Acad. Sci. USA **103**, 7222 (2006).
[2] E. Evans, Annu. Rev. Biophys. Biomol. Struct. **30**, 105 (2001).
[3] R. Merkel, P. Nassoy, A. Leung, K. Ritchie, and E. Evans, Nature (London) **397**, 50 (1999).
[4] J. Wen, M. Manosas, P. Li, S. Smith, C. Bustamante, F. Ritort, and I. Tinoco Jr., Biophys. J. **92**, 2996 (2007).
[5] S. Block, C. Asbury, J. Shaevitz, and M. Lang, Proc. Natl. Acad. Sci. USA **100**, 2351 (2003).
[6] A. Clemen, M. Vilfan, J. Jaud, J. Zhang, M. Bärmann, and M. Rief, Biophys. J. **88**, 4402 (2005).
[7] J. Laakso, J. Lewis, H. Shuman, and E. Ostap, Science **321**, 133 (2008).
[8] M. Nöllmann, M. Stone, Z. Bryant, J. Gore, N. Crisona, S. Hong, S. Mitelheiser, A. Maxwell, C. Bustamante, and N. Cozzarelli, Nat. Struct. Mol. Biol. **14**, 264 (2007).
[9] S. Leuba, M. Karymov, M. Tomschik, R. Ramjit, P. Smith, and J. Zlatanova, Proc. Natl. Acad. Sci. USA **100**, 495 (2003).
[10] Y. F. Chen, J. N. Milstein, and J. C. Meiners, Phys. Rev. Lett. **104**, 258103 (2010).
[11] B. Marshall, M. Long, J. Piper, T. Yago, R. McEver, and C. Zhu, Nature (London) **423**, 190 (2003).
[12] E. Evans and K. Ritchie, Biophys. J. **72**, 1541 (1997).
[13] I. Tinoco Jr. and C. Bustamante, Biophys. Chem. **101**, 513 (2002).
[14] W. Greenleaf, M. Woodside, E. Abbondanzieri, and S. Block, Phys. Rev. Lett. **95**, 208102 (2005).
[15] J. Gebhardt, T. Bornschlögl, and M. Rief, Proc. Natl. Acad. Sci. USA **107**, 2013 (2010).
[16] M. Manosas and F. Ritort, Biophys. J. **88**, 3224 (2005).
[17] M. Manosas, A. Mossa, N. Forns, J. Huguet, and F. Ritort, J. Stat. Mech.: Theory Exp. (2009) P02061.
[18] N. Forns, S. de Lorenzo, M. Manosas, K. Hayashi, J. Huguet, and F. Ritort, arXiv:1105.4734.
[19] M. Kireeva, B. Hancock, G. Cremona, W. Walter, V. Studitsky, and M. Kashlev, Mol. Cell **18**, 97 (2005).

[20] V. Bondarenko, L. Steele, A. Ujvári, D. Gaykalova, O. Kulaeva, Y. Polikanov, D. Luse, and V. Studitsky, Mol. Cell **24**, 469 (2006).
[21] C. Hodges, L. Bintu, L. Lubkowska, M. Kashlev, and C. Bustamante, Science **325**, 626 (2009).
[22] E. Galburt, S. Grill, A. Wiedmann, L. Lubkowska, J. Choy, E. Nogales, M. Kashlev, and C. Bustamante, Nature (London) **446**, 820 (2007).
[23] D. Wales, Mol. Phys. **100**, 3285 (2002).
[24] S. Mehraeen, B. Sudhanshu, E. F. Koslover, and A. J. Spakowitz, Phys. Rev. E **77**, 061803 (2008).
[25] G. Li, M. Levitus, C. Bustamante, and J. Widom, Nat. Struct. Mol. Biol. **12**, 46 (2004).
[26] T. Richmond and C. Davey, Nature (London) **423**, 145 (2003).
[27] B. Sudhanshu, S. Mihardja, E. Koslover, S. Mehraeen, C. Bustamante, and A. Spakowitz, Proc. Nat. Acad. Sci. USA **108**, 1885 (2011).
[28] H. Wang, C. Peskin, and T. Elston, J. Theor. Biol. **221**, 491 (2003).
[29] G. Lattanzi and A. Maritan, J. Chem. Phys. **117**, 10339 (2002).
[30] S. Mehraeen and A. Spakowitz, Phys. Rev. E (in press), (2012).
[31] D. Gillespie, J. Phys. Chem. **81**, 2340 (1977).
[32] L. Liu and J. Wang, Proc. Natl. Acad. Sci. USA **84**, 7024 (1987).